

# Acetylides of cycloplatinated ferrocenylamines; synthesis and redox chemistry†

C. John McAdam, Evan J. Blackie, Joy L. Morgan, Sarah A. Mole, Brian H. Robinson and Jim Simpson

Department of Chemistry, University of Otago, P.O. Box 56, Dunedin, New Zealand

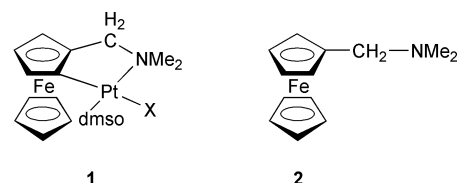
Received 23rd February 2001, Accepted 13th June 2001

First published as an Advance Article on the web 2nd August 2001

Sonogashira coupling of a terminal alkyne with cycloplatinated ferrocenylamine complexes gave the acetylides  $\text{Pt}\{\text{[RC}\equiv\text{C][Me}_2\text{NCH}_2(\sigma\text{-Fc)}\}\text{dmsO}$ , which were characterised by analysis, spectroscopy and, for the  $\text{R} = \text{SiMe}_3$ , **3**, **5** complexes, X-ray structural analyses. A butadiyne complex was also isolated in reactions of **3**. Equivalent reactions with LDA led to an unusual deplatination reaction to give the ethynylferrocenylamine. The  $\text{Pt(II)}$  centre functions as a redox switch at  $E^{+/0} = -0.21$  V and the spectroscopic and electrochemical data show that the acetylide is a  $\pi$ -donor ligand. There is a strict delineation of the electronic requirements for the *trans* Pt–N and *trans* Pt–C(Cp) groups in these cycloplatinated compounds. Oxidation of **3** gives rise to low energy bands based on the  $\text{Pt(II)}$  unit; an additional broad band at 1100 nm occurs in  $5^+$  but not  $5^{2+}$ .

Molecules with ethynyl functionalities provide a route to a myriad of structures which give the opportunity for redox centres to ‘talk’ to each other through the rigid  $\sigma$ -acetylide links.<sup>1</sup> This communication is important if there is to be efficient energy transfer for molecular wires or photonic relays. Ethynylferrocenyl derivatives are particularly attractive because the redox centre is well-behaved and synthetic elaboration of the local ferrocenyl environment is relatively straightforward. The redox potential of the ferrocenyl moiety can be tuned by appropriate substitution on the cyclopentadienyl ring.<sup>2</sup> Nevertheless, even with ring substitution, the potential only varies by about 0.5 V. In contrast, low-valent metal clusters offer a window of +0.8 V to –1.2 V,<sup>3</sup> although they are nowhere near as robust. For our work on switchable fluorescent materials we required a redox centre with an oxidation potential close to zero. Furthermore, it was preferable for the redox centre to have a structural pivot that would lead to predetermined geometries such as molecular squares. A group of molecules that satisfy these criteria are the cycloplatinated ferrocenylamines **1** ( $\text{X} =$  anionic halide). They are readily prepared from the ferrocenylamine **2**, kinetically stable in air and are oxidised at very low potentials.<sup>4,5</sup> Their square planar geometry is ideally suited to molecular square formation, although the specific electronic demands on the *trans* –NMe<sub>2</sub> and *trans* Pt–C positions (good  $\pi$ -acceptor and donor anion, respectively<sup>5,6</sup>) restrict the choice of linkages for the sides. Replacement of the anionic halide  $\text{X}$  *trans* to the Pt–C bond by a donor acetylide group would give greater synthetic flexibility and a communication link. This type of compound is the principal target molecule in the work described in this paper.

During preliminary work on this system,<sup>7</sup> it was observed that a deplatination reaction appeared to take place when a terminal acetylene was reacted with **1**, the product being an ethynyl derivative of the ferrocenylamine **2**. This type of derivative has been reported by Schlögl and co-workers<sup>8</sup> and the *ortho*-directing character of the  $\text{CH}_2\text{NMe}_2$  substituent has been used to make, selectively, 1,2-ethynyl derivatives and oligomers.<sup>9</sup> Related chiral 1,2-ethynyl derivatives with a  $\text{CH}(\text{Me})\text{NMe}_2$



amino substituent have also been reported.<sup>10</sup> Because the  $\text{CH}_2\text{NMe}_2$  substituent is a strong base, the redox chemistry of these compounds is a function of pH.<sup>11</sup> Consequently, elaboration of the ethynyl linkage in derivatives of **2** could generate pH dependent molecular switches.<sup>12</sup> We therefore explored conjointly with reactions of **1** the scope of the deplatination reaction and properties of both cycloplatinated and non-platinated ethynylferrocenyl derivatives.

## Results and discussion

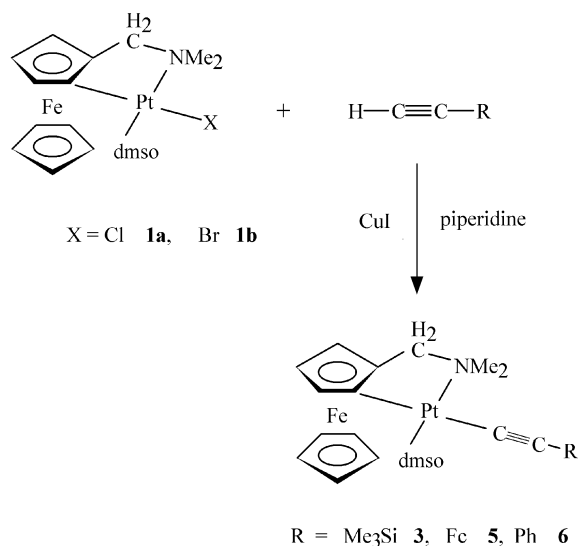
The most convenient and high yielding synthesis of acetylide derivatives of cycloplatinated ferrocenylamines is *via* a Sonogashira  $\text{CuI}$ -catalysed reaction with **1b**. Trimethylsilyl **3**, ferrocenyl **5**, and phenyl **6** derivatives were prepared *via* this route (Scheme 1). Reactions with **1a**, where a chloro group is in the *trans* Pt–C position, also gave the same products but in lower yields.

Under Sonogashira conditions, the reaction of **1a** with trimethylsilylacetylene led to partial desilylation of **3**, with consequent formation of the butadiyne **4** (Scheme 2).

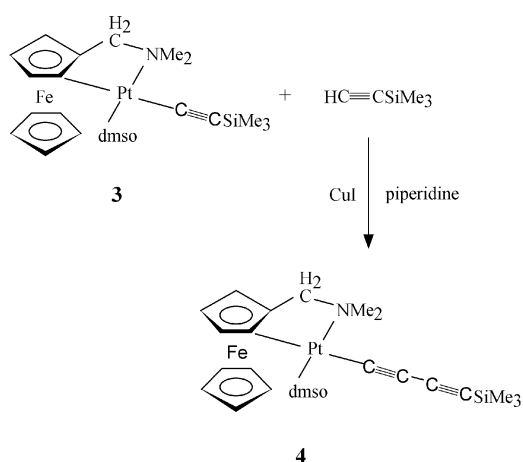
Alternative routes attempted—the prior removal of the halide from **1** with a  $\text{Ti[I]}$  salt<sup>13</sup> or using a triflate derivative of **1**—were unsuccessful. However, reaction of **1b** with trimethylsilylacetylene or phenylacetylene in the presence of LDA (lithium diisopropylamide) gave **3** and **6**, respectively, in relatively poor yield (Scheme 3).

An unexpected deplatination of **1a** to give 1-dimethylaminomethyl-2-phenylethynylferrocene **7**, was observed with phenylacetylene in the presence of LDA (Scheme 4). Although a similar deplatination reaction occurred with ethynylacetylenes it was not reproducible. For reference, the other functionalised ferrocenylamines **8** and **9**<sup>10</sup> were directly synthesised from 1-dimethylaminomethyl-2-iodoferrocene **10** (Scheme 5). The mechanism for the deplatination step is problematical.

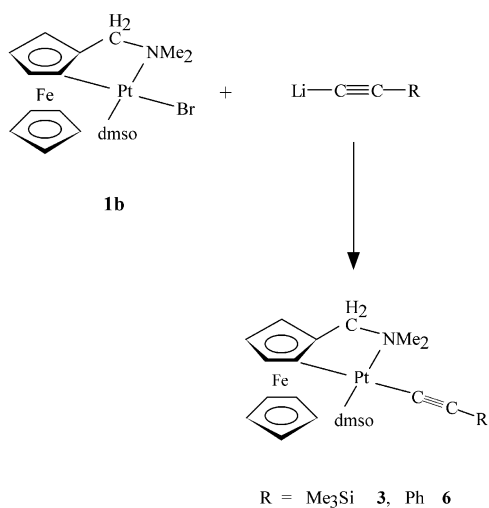
† Electronic supplementary information (ESI) available: rotatable 3-D crystal structure diagram in CHIME format. See <http://www.rsc.org/supdata/dt/bl/b101776o/>



**Scheme 1**

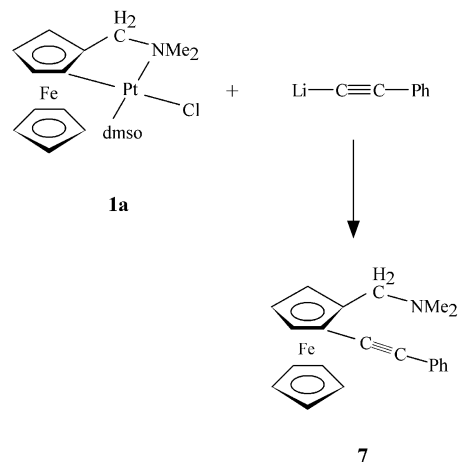


**Scheme 2**

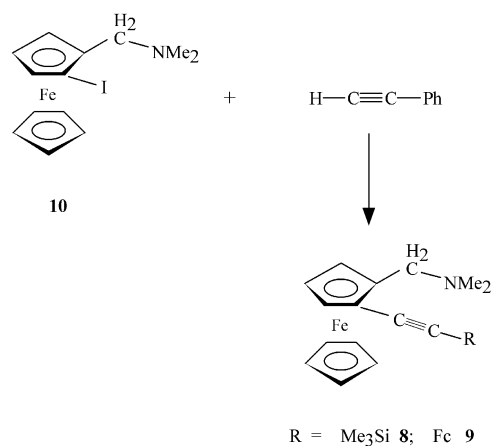


**Scheme 3**

Oxidatively-induced reductive elimination facilitated by electron-donor substituents on the Pt(II) centre has been demonstrated for *cis*-aryl(ferrocenylacetylide)Pt complexes<sup>14</sup> but reductive elimination necessitates a *cis* stereochemistry.<sup>15</sup> Previous work has shown<sup>4</sup> that the Pt–C bond in **1** is not attacked by electrophiles or nucleophiles; moreover, although insertion with cyclopalladated species is well known,<sup>16</sup> we have not been able to induce the insertion of alkynes into the Pt–C bond. Pertinent to our system is that demetalation of cyclopalladated ferrocenyl



**Scheme 4**



**Scheme 5**

compounds containing two inserted diphenylacetylenes to give carbocycles can be achieved<sup>17</sup> by treatment with a neutral coordinating ligand. A similar route may be responsible for the depletion.

The acetylide derivatives were fully characterised by elemental analysis, IR, <sup>1</sup>H, <sup>13</sup>C and, where appropriate, <sup>195</sup>Pt NMR spectroscopy. Spectroscopic data for **7–9** were unremarkable. Diastereotopic resonances for both the NMe<sub>2</sub> and dmsol groups in the <sup>1</sup>H NMR of **3–6** show that ring stereochemistry was maintained, although the difference in chemical shift is smaller than in **1**. The ν(C≡C) modes for **3–5** are typical of a σ,η<sup>1</sup>-acetylide group bound to a metal, with their energy dependent on the acetylide terminal substituent. Two coupled ν(C≡C) modes for **4** at 2172 and 2126 cm<sup>−1</sup> are also consistent with a σ,η<sup>1</sup>-diethynyl structure. A puzzling observation was the *two* ν(C≡C) bands at 2113 and 2097 cm<sup>−1</sup> obtained reproducibly in both the solution and solid spectra of **5**, whereas the PPh<sub>3</sub> analogue **11** (generated by the direct reaction of **5** with PPh<sub>3</sub> in CH<sub>2</sub>Cl<sub>2</sub>) has only one band at 2074 cm<sup>−1</sup>.

Theoretical calculations, spectroscopic and X-ray data of η<sup>1</sup>-alkynyl ligands bound to platinum suggest<sup>18</sup> that these ligands are good σ- and π-donors but poor π-acceptors. In η<sup>1</sup>-alkynyl phosphine derivatives the electron population of π\*(C≡CR) is <0.05 e with strong destabilising interactions between the occupied π-metal and π(C≡CR) orbitals. These electronic factors are reflected in the <sup>195</sup>Pt NMR data for **3–6**, where the chemical shifts follow the relative π-donor capability of the anions. Thus, the <sup>195</sup>Pt chemical shift is between −3700 and −3725, irrespective of the acetylide substituent, similar to that for the acetato (−3692<sup>13</sup>), but significantly upfield from **1a** and **1b** (−3763 and −3815 respectively<sup>4</sup>). The <sup>13</sup>C{<sup>1</sup>H} NMR spectra of **3** shows signals due to the α- and β-alkynyl carbons at 148.7 and 107.4 ppm. <sup>1</sup>J(C–Pt) coupling to the α-alkynyl

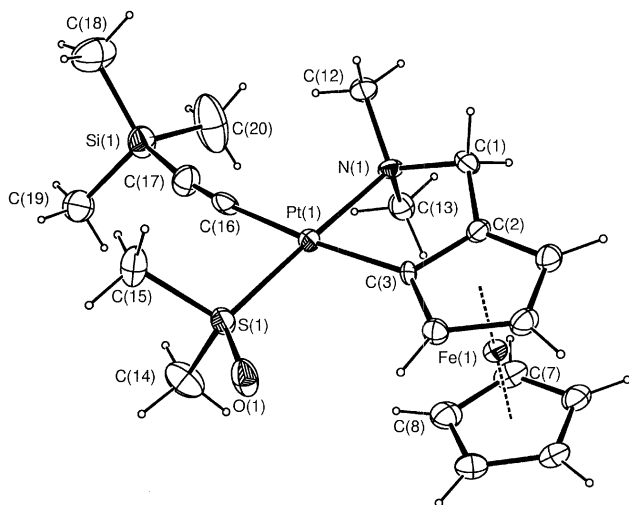


**Fig. 1** Perspective view of **3** showing the atom numbering scheme with thermal ellipsoids drawn at the 50% probability level. For clarity only the first two atoms of consecutively numbered cyclopentadienyl rings are labelled.

carbon atoms was 920 Hz. For comparison,  $^1J(\text{C-Pt})$  coupling to the cyclometallated C atoms of the ferrocenyl moiety was 790 Hz. Similar observations were made by Osakada *et al.*<sup>19</sup> for the complex  $\text{Pt}(p\text{-C}_6\text{H}_4\text{OMe})(\text{C}\equiv\text{CPh})(\text{PET}_3)_2$  which had  $^1J(\text{C-Pt})$  values of 890 Hz for the metal bound alkyne carbon and 673 Hz for the coordinated arene C atom. They interpreted this finding to support the partial contribution of a vinylidene structure to the Pt-alkynyl bond; equally the findings are consistent with an acetylide functioning as a good  $\pi$ -donor. However, since such coupling constants are significantly dependent on the Fermi contact interaction and therefore the s-character in the Pt-C bonds<sup>20</sup> (albeit modified by relativistic effects in the case of heavy nuclei such as Pt), the direct and uncompensated comparison of coupling constants involving alkyne (sp) and arene (sp<sup>2</sup>) carbon atoms must be viewed with some caution. It is noteworthy in this context that the trends in Pt-C (alkyne) and Pt-C (arene) bond distances observed for **3** are the complete reverse of those for  $\text{Pt}(p\text{-C}_6\text{H}_4\text{OMe})(\text{C}\equiv\text{CPh})(\text{PET}_3)_2$ , *vide infra*. This further suggests that factors other than the degree of back-bonding in the Pt-C vector contribute significantly to the observed coupling constants.

To give us a comparative structural basis for a discussion of the electronic characteristics of the acetylide ligand in these cycloplatinated complexes, and to seek a structural explanation for the anomalous  $\nu(\text{C}\equiv\text{C})$  spectrum of **5**, X-ray structural analyses were carried out on **3** and **5**.

#### X-Ray structures of **3** and **5**

For **3**, the crystals comprise unique molecules of **3** together with benzene solvate in the monoclinic unit cell. For **5**, the monoclinic unit cell contains molecules of **5** together with two water molecules, both at approximately 50% occupancy. Perspective views of **3** and **5** are shown in Fig. 1 and 2, respectively. These figures define the atom numbering schemes used. Selected bond length and angle data for both molecules appear in Table 1.

For **3** and **5** the coordination spheres of the platinum atoms comprise the S(1) atoms of S-bound dmsoligands *trans* to the amine N(1) atoms of the orthometallated ferrocenylamine ligands. The Pt-bound C(3) atom of the substituted cyclopentadienyl ring is *trans* to the C(16) atom of the terminally bound trimethylsilylacetylide for **3** and ferrocenylacetylide for **5**. These occupy the fourth coordination site in each case. The N(1) and C(3) atoms are the donors in five-membered chelate rings formed by the orthometallated ferrocenylamine ligands in both molecules. Some deviation from the idealised square planar geometry about Pt is apparent with the angles C(3)-Pt-C(16)

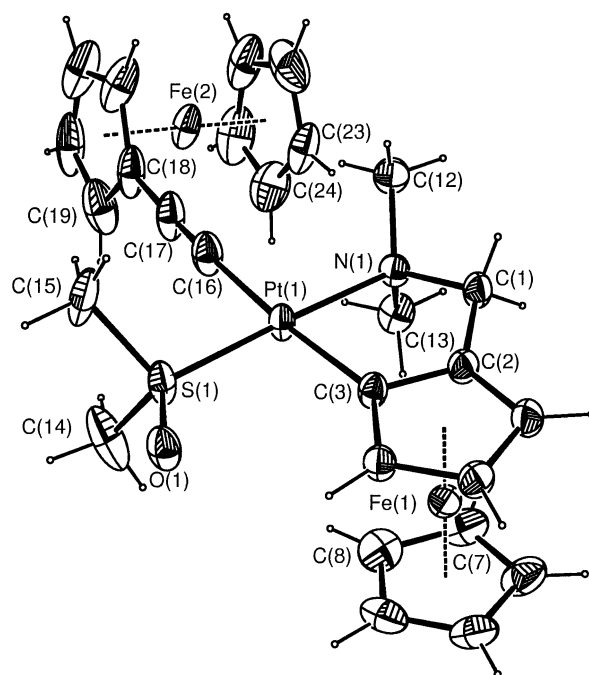


**Fig. 2** Perspective view of **5** showing the atom numbering scheme with thermal ellipsoids drawn at the 50% probability level. For clarity only the first two atoms of consecutively numbered cyclopentadienyl rings are labelled.

**Table 1** Selected bond lengths (Å) and angles (°) for **3** and **5**

	<b>3</b>	<b>5</b>
Pt(1)-C(3)	2.031(5)	2.023(5)
Pt(1)-C(16)	2.076(5)	2.059(6)
C(16)-C(17)	1.164(8)	1.191(8)
C(17)-Si(1)	1.838(6)	
C(17)-C(18)		1.447(8)
Pt(1)-S(1)	2.1853(13)	2.1912(14)
Pt(1)-N(1)	2.137(4)	2.141(4)
N(1)-C(1)	1.505(7)	1.510(7)
C(1)-C(2)	1.495(7)	1.495(7)
C(2)-C(3)	1.424(7)	1.438(7)
Fe(1)-C(2-6) mean	2.05(2)	2.067(18)
Fe(1)-C(7-11) mean	2.042(5)	2.055(8)
Fe(2)-C(18-22) mean		2.051(13)
Fe(2)-C(23-27) mean		2.039(15)
C(3)-Pt(1)-N(1)	82.10(18)	82.72(18)
C(16)-Pt(1)-N(1)	90.26(17)	90.03(19)
C(3)-Pt(1)-S(1)	97.61(15)	96.68(14)
C(16)-Pt(1)-S(1)	89.91(14)	90.47(16)
C(3)-Pt(1)-C(16)	171.9(2)	172.4(2)
N(1)-Pt(1)-S(1)	177.63(12)	177.34(13)
C(17)-C(16)-Pt(1)	173.5(5)	175.4(5)
C(16)-C(17)-Si(1)	170.2(6)	
C(16)-C(17)-C(18)		177.7(6)

171.9(2)° for **3** and 172.4(2)° for **5** with S(1)-Pt(1)-N(1) 177.63(12)° for **3** and 177.34(13)° for **5**. Deviations from the PtL<sub>4</sub> ring plane for **3** range from -0.0391(17) Å for Pt(1) to 0.0061(18) Å for S(1) while for **5**, the corresponding range is -0.0371(19) Å for Pt(1) to 0.006(3) Å for C(16). The Pt-N (2.137(4) Å for **3**, 2.141(4) Å for **5**) and Pt-S (2.1853(13) Å for **3**, 2.1912(14) Å for **5**) distances are similar to those found in related compounds.<sup>4-6,13</sup> The Pt-C(3) bond to the metallocene ring is significantly longer, 2.031(5) Å for **3** and 2.023(5) Å for **5**, than the corresponding distances in the closely related compounds  $[\text{Pt}\{\sigma\text{-}\eta^5\text{-C}_5\text{H}_3\text{CH}_2\text{NMe}_2\}\text{Fe}(\eta^5\text{-C}_5\text{H}_5)\}(\text{dmsol})\text{X}]$ , (X = Cl,<sup>4</sup> O<sub>2</sub>CCH<sub>3</sub>)<sup>13</sup> where the comparable bond lengths were 1.988(7) Å and 1.976(8) Å, respectively. Furthermore, the Pt-C(16) (alkyne) bonds, 2.076(5) Å for **3** and 2.059(6) Å for **5**, are longer than the Pt-C(3) (Cp) bonds, a variation that may reflect

the competitive *trans* influence across the coordination spheres of the Pt atoms. In *trans*-bis(alkyne) platinum complexes the Pt–C(alkyne) bond distance is generally close to 2.00 Å.<sup>21</sup> However, to our knowledge, no comparable data exist on compounds with  $\sigma$ -bound cyclopentadienyl rings *trans* to Pt-substituted alkynes but, given the similarity between the  $\eta^5$ -C<sub>5</sub> ring compounds and arenes, comparison with *trans*-Pt–arene systems may be useful. An extensive structural investigation, comparing Pt–Cl bond extension in *trans*-alkynyl–Pt–Cl *vs* *trans*-arene–Pt–Cl complexes, revealed that arenes have a greater *trans* influence than alkynyl ligands.<sup>18</sup> The bond lengths reported here show a similar trend. However, structural data from a variety of *trans*-alkynyl–Pt–arene complexes show that this trend is exclusively, and often significantly, reversed.<sup>22</sup> A similar effect is also noted in analogous Pd compounds and partial contribution of a vinylidene structure has been cited as an explanation.<sup>19</sup> There is, however, no evidence for such reversal in the molecules reported here as, in addition to the long Pt(1)–C(3) bonds for both **3** and **5**, the C≡C bond lengths, 1.164(8) Å for **3** and 1.191(8) Å for **5**, are somewhat short in comparison to the mean C≡C distance of 1.201(16) Å observed for a range of L<sub>n</sub>M–C≡C–R (R = C or Si) compounds.<sup>18</sup> Clearly in both cases, either the arene/cyclopentadienyl comparison is inappropriate, or the stereochemical consequences of chelate ring formation in the cyclometallated complexes have a significant influence on the Pt–C(Cp) and Pt–C(alkyne) vectors. We would favour the latter explanation.

The cyclopentadienyl rings in the orthometallated ferrocene moieties adopt an approximately eclipsed conformation, with the mean torsion angle C(m)–C(1g)–C(2g)–C(n) of 1.21(1)° for **3** and 1.2(2)° for **5** (C(m) = C(2)–C(6), C(n) = C(7)–C(11) and C(1g) and C(2g) are the corresponding ring centroids). The dihedral angle between the planes of the orthometallated Cp rings is 7.5(5)° for **3** and 5.4(5)° for **5**. The average Fe–C distances (2.05(2) Å for **3**, 2.06(1) for **5**) are not unusual and the Fe atom is almost equidistant from each of the Cp rings in both molecules (1.653(2) Å and 1.647(3) Å for **3**; 1.666(3) Å and 1.660(3) Å for **5**).<sup>23</sup> An approximately eclipsed conformation is also displayed by the ferrocene of the ferrocenylacetylide ligand with the mean torsion angle 5(3)°, as detailed above. The average Fe–C distance is 2.05(1) and the Fe(2) atom lies 1.651(3) Å and 1.653(3) Å, respectively, from the Cp rings. The interplanar angle between the Cp rings of this pendant ferrocenyl (1.76(5)°) is significantly smaller than those for the cyclometallated ferrocenyl rings in both **3** and **5**. This may further reflect steric interactions in the cyclometallated system arising from the formation of the chelate ring.

## Redox chemistry

### Electrochemistry

Previous workers have<sup>9</sup> experienced difficulties in measuring the electrochemistry of 1-ethynyl-3-dimethylaminoferrocenes. This was attributed to oxidation of the amino functionality,<sup>24</sup> although it is just as likely that protonation caused the broad *i/V* responses.<sup>11</sup> The protonated chiral analogues of Long and co-workers<sup>10</sup> gave sensible *i/V* responses but the deprotonated compounds were unstable. Not surprisingly, the *i/V* responses for **7–9** were broader, due to facile protonation, whereas **3–6** displayed Nernstian kinetics.

All compounds in our work with a single ferrocenyl centre fortunately gave the normal<sup>2,5</sup> cyclic and square-wave voltammograms in CH<sub>2</sub>Cl<sub>2</sub> of a chemically-reversible one-electron [Fc]<sup>+/0</sup> couple (potentials are referenced to decamethylferrocene at 20 °C). Deprotonated **2** is oxidized at 0.55 V<sup>11</sup> and **1a** and **1b** at 0.33 V and 0.34 V, respectively.<sup>4,7</sup> An ethynyl group normally acts as an electron-withdrawing substituent and the anodic shift between ferrocene and ethynylferrocene is 0.16 V. This indeed is the anodic difference between *E*<sup>0+</sup>[**2**] and its ethynyl derivatives

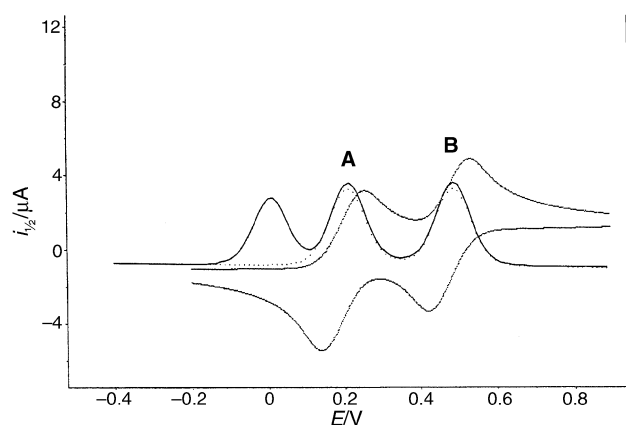
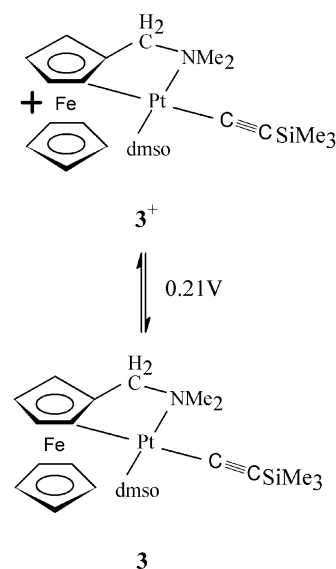


**Fig. 3** Square-wave and cyclic voltammograms of **5** in CH<sub>2</sub>Cl<sub>2</sub>, 15 Hz (sweep rate) 200 mV s<sup>−1</sup>, Pt, 20 °C; referenced to decamethylferrocene at 0.0 V.

**7–9**; for example, *E*<sup>0+</sup>[**2**] + 0.16 V = 0.71 V, close to *E*<sup>0+</sup> [**7**] at 0.70 V. This demonstrates the well-illustrated principle that the *E*<sup>0+</sup> potentials for most ferrocenyl compounds can be calculated from the relationship, *E*<sup>0+</sup> [Fc] = 0.55 V plus Σ( $\delta_a$ ), where  $\delta_a$  is a substitution parameter for each component.<sup>6,24</sup>

Surprisingly, substitution of a halide ion in the cycloplatinated compounds by the acetylide anion causes a large *cathodic* shift in the potential for the oxidation of the ferrocenyl component of the PtNSL( $\sigma$ -CFc) square planar unit (Scheme 6).



**Scheme 6**

For example, *E*<sup>0+</sup> [**3**] = 0.21 V, a difference of 0.12 V from *E*<sup>0+</sup> [**1a**]. We have found<sup>7</sup> that  $\sigma$ -donor substituents *trans* to the Pt–C bond with little  $\pi$ -donor characteristics have little influence on *E*<sup>0+</sup> for cycloplatinated species, whereas the opposite is true for the *trans* Pt–N  $\pi$ -acceptor groups *trans* to the NMe<sub>2</sub> substituent. The cathodic shift, together with the <sup>195</sup>Pt NMR data for **3–6** and theoretical calculations for related systems,<sup>18</sup> are consistent with the acetylide anion acting as a  $\pi$ -donor. It is intriguing that the  $\pi$ -donor and  $\pi$ -acceptor ligand requirements around the cycloplatinated unit are specific and directional. Presumably, the orbital symmetry and coefficients of the Pt–C bond are the parameters which are dictating the electronic configuration about the Pt(II) ion.

The complexes in which there are two ferrocenyl redox centres, **5** and **9**, give an insight into the possible electronic interaction between the non-equivalent ferrocenyl redox centres linked *via* a C≡C bond. **5**, displays two reversible one-electron steps A, B in the cyclic and square-wave voltammetry (Fig. 3).

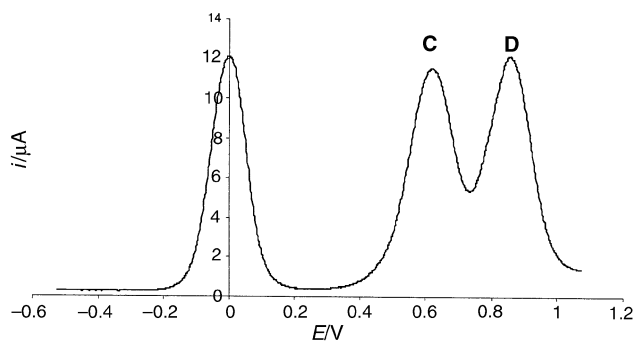
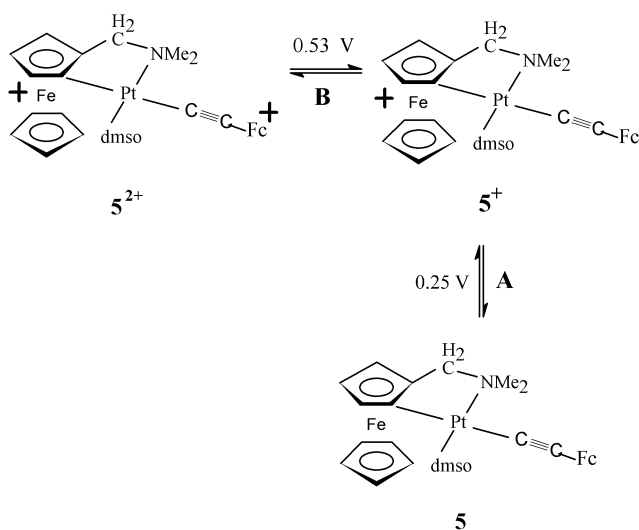


**Fig. 4** Square-wave voltammogram of **8** in  $\text{CH}_2\text{Cl}_2$ , 15 Hz, Pt, 20 °C; referenced against decamethylferrocene at 0.0 V.

$E^{0/+}[\text{A}] = 0.25$  V, is close to  $E^{0/+}[\text{3}]$  and is therefore assigned to the unperturbed cycloplatinated redox centre. Cycloplatination shifts a  $E^{0/+}[\text{Fc}]$  couple cathodically by  $\sim 0.2$  V.<sup>7</sup> As  $E^{0/+} = 0.71$  V for  $\text{HC}\equiv\text{CFc}$  we would expect  $E^{0/+}$  for a 'Pt' $\text{C}\equiv\text{CFc}$  unit to be  $\sim 0.51$  V, remarkably close to  $E^{0/+}[\text{B}]$  at 0.53 V for **5** (Scheme 7).



**Scheme 7**

If there was significant interaction between the cycloplatinated and terminal ferrocenyl redox centres oxidation of the former at the first redox centre, **A**, would make it more difficult to oxidise the second ferrocenyl redox centre, **B**. The observation that the potentials for **A** and **B** are similar to those for analogous isolated redox centres shows that there is minimal communication between them. This conclusion was supported by the observation that substitution of dmso by  $\text{PPh}_3$  in the *trans* Pt–N position, complex **11**, gave  $E^{0/+} = 0.20$  V and 0.48 V for **A** and **B**, respectively. The small cathodic shift when dmso is replaced by a better donor is similar to that for non-acetylide complexes.<sup>4</sup>

The situation for the non-cycloplatinated complex **9** is different. In this case, two one-electron processes are observed in the cyclic and square-wave voltammograms (Fig. 4), **C** ( $E^{0/+} = 0.62$  V, reversible) and **D** ( $E^{0/+} = 0.86$  V, quasi-reversible), neither of which corresponds to the potentials for unperturbed parent redox centres. **C** is assigned to the dimethylaminomethylferrocenyl redox centre shifted from  $E^{0/+}$  for the  $\text{Me}_3\text{Si}$  analogue by the electron donating  $\text{FcC}\equiv\text{C}-\text{Cp}$  ring substituent. The coulombic effect of the oxidation of the ferrocenylamine then causes an anodic shift of  $E^{0/+}[\text{FcC}\equiv\text{C}-]$  giving rise to **B** at 0.86 V (Scheme 8). That is, the ethynyl link in **9** provides a bridge for communication, and hence inductive and coulombic perturbation of the redox centres, which is not available with an acetylide link in **5**.

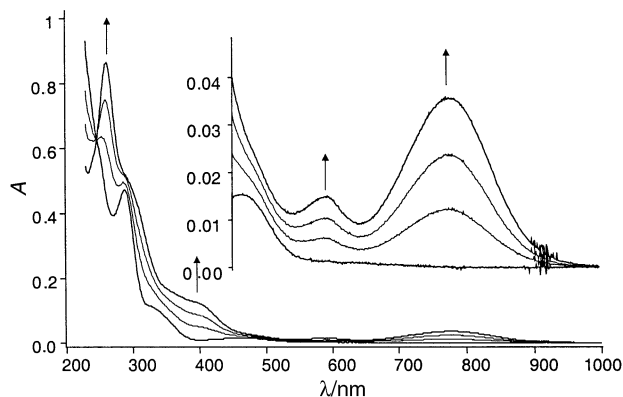
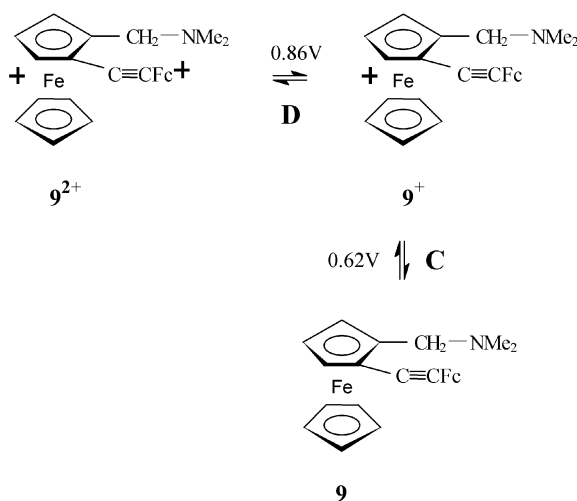


**Fig. 5** OTTLE UV/VIS spectra of **3** in  $\text{CH}_2\text{Cl}_2$ ; arrows indicate increasing absorbance as the voltage is increased to **A**, the first redox process.



**Scheme 8**

### Electronic spectra

The electronic spectra of cycloplatinated derivatives of **1** are characterised<sup>7</sup> by two absorptions, 450–470 nm ( $\epsilon \sim 600$ ), and  $<350$  nm ( $\epsilon > 1000$ ). Both bands are similar in energy and intensity to those found in other ferrocene compounds.<sup>25</sup> They are of little diagnostic value as their energies are relatively invariant to changes in the Pt(II) coordination sphere. However, significant changes to the electronic spectra take place upon oxidation of the cycloplatinated acetylides. One-electron oxidation of **3** at 0.21 V gave rise to the new spectrum shown in Fig. 5 with a well-defined isosbestic point at 246 nm. Reduction of **3**<sup>+</sup> gave the original spectrum, showing that only one long-lived species is formed on oxidation. The high energy (320 nm,  $\epsilon = 2500$ ) and low energy (464 nm,  $\epsilon = 340$ ) 'ferrocenyl' bands in **3** are red-shifted to 395 nm ( $\epsilon = 1320$ ) and  $\sim 480$  nm (shoulder,  $\epsilon \sim 540$ ) respectively in **3**<sup>+</sup>. Similar red-shifts are observed upon the oxidation of **1a** and **1b**, confirming that the acetylide group does not perturb the HOMO–LUMO levels of the Pt(II) coordination sphere. The new weak band for **3**<sup>+</sup> at 590 nm ( $\epsilon = 500$ ) could be assigned to a Fe-centred SOMO ( $e_{2g}$ )  $\rightarrow$  LUMO transition (normally found at  $\sim 630$  nm in ferrocenium compounds). The other new band, a broad low energy absorption at 780 nm ( $\epsilon = 770$ ), is assigned to a MCLT transition centred on the Pt(II) unit. Precise assignments must await theoretical and Raman studies underway at present but, to our knowledge, this is the first report of low-energy electronic transitions in either neutral or oxidised, cycloplatinated or cyclopalladated complexes. One-electron oxidation of **5** to **5**<sup>+</sup>, a complex which has two ferrocenyl redox centres, gave essentially the same absorption profile as **3**<sup>+</sup> (Fig. 6). There is a small red-shift in the

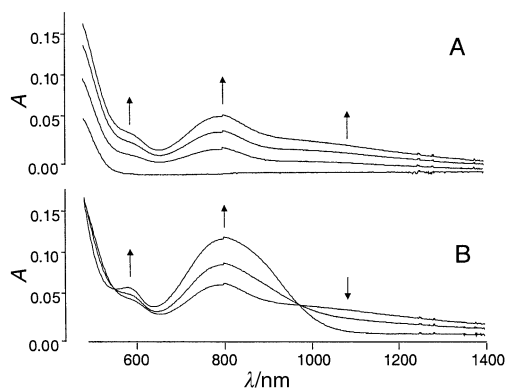


**Fig. 6** OTTLE UV/VIS spectra of **5** in  $\text{CH}_2\text{Cl}_2$ ; arrows indicate increasing absorption as the voltage is increased: (A) the first oxidation potential and (B) the second oxidation potential.

weak 600 nm, ( $\epsilon = 300$ ) and 800 nm ( $\epsilon = 540$ ) bands from those in  $3^+$  and the high (345 nm,  $\epsilon = 1610$ ) and lower energy (456 nm,  $\epsilon = 538$ ) ferrocenyl bands effectively merge to give a broad unresolved absorption. These observations are consistent with the electrochemical assignment in Scheme 7, in which the first redox process is centred on the cycloplatinated ferrocenyl unit. What was unexpected for  $5^+$ , given that the electrochemical data did not support interaction between the two redox centres, was the very broad band in the near-infrared at  $\sim 1100$  nm ( $\epsilon = 484$ ) which has a profile typical of an IT transition (Fig 6). If it is an IT transition, some mixing of the Pt( $\pi$ ) unit and pendant ferrocenyl orbitals must occur but more work is required to determine its origin. Oxidation of the pendant ferrocenyl group to give  $5^{2+}$  eliminated the 1100 nm band and caused a blue-shift of the 600 nm band to 587 nm ( $\epsilon = 925$ ) and both this band and that at 801 nm ( $\epsilon = 1960$ ) to gain significant intensity. The isosbestic point 985 nm confirms that only two species are involved in the transformation from  $5^+$  to  $5^{2+}$ . Since the 587 nm and 800 nm bands are characteristic of the  $\text{C}\equiv\text{CFe}^+$  unit, the electronic spectrum of  $5^+$  gives credence to the notion that there is little orbital interaction between the two ferrocenyl redox centres.

## Conclusion

Successful syntheses have been developed for cycloplatinated ferrocenylamine-acetylides. The same strategy could be used to make chiral analogues and molecules with two platinated groups per ferrocene. These newly developed syntheses provide the platform for incorporation of the easily oxidised cycloplatinated redox centre into dendrimers and other molecular architectures. For example, structures in which the cycloplatinated ferrocenyl unit acts as a linker to fluorophores have been made in these laboratories. There are two important electronic considerations when designing these structures. First, the acetylide in the *trans* Pt–C position must be a good  $\pi$ -donor, with the ligand in the *cis* position a good  $\pi$ -acceptor. This separability could be exploited to direct energy flow in specific directions. Second, there does not appear to be effective interaction or energy flow across the acetylide bridge; that is, the acetylide is an insulator. While this is not necessarily important for sensors, it is for molecular wire development. In contrast, the non-platinated dimethylaminoferrocenes do provide the communication and, an added bonus, pH control of potential, but they are less robust. The observation of low-energy electronic transition in the oxidised cycloplatinated complexes has important consequences for use of these complexes as redox switches when linked to fluorophores and these are being investigated at present.

## Experimental

Solvents were dried and distilled by standard procedures, and

all reactions were performed under nitrogen. **1**,<sup>4</sup> ethynylferrocene,<sup>26</sup> and **10**<sup>27</sup> were prepared by literature methods. Commercial reagents were used as received. IR spectra were recorded on a Perkin-Elmer Spectrum BX FT-IR, NMR on a Varian VXR300 MHz or Gemini 200 MHz (proton decoupled <sup>195</sup>Pt spectra were referenced to  $\text{K}_2\text{PtCl}_4$ ) and electronic spectra on a Jasco V 550 UV/VIS. Microanalyses were carried out by the Campbell Microanalytical Laboratory, University of Otago. Mass spectra were recorded on a Kratos MS80RFA instrument with an Iontech ZN11NF atom gun. Cyclic and square-wave voltammetry in  $\text{CH}_2\text{Cl}_2$  were performed for all compounds using a three-electrode cell with a polished disk, Pt (2.27 mm<sup>2</sup>) as the working electrode; solutions were  $\sim 10^{-3}$  M in electroactive material and 0.10 M in supporting electrolyte (triply recrystallised TBAPF<sub>6</sub>). Data were recorded on an EG & G PAR 273A computer-controlled potentiostat. Scan rates of 0.05–1 V s<sup>−1</sup> were typically employed for cyclic voltammetry and for Osteryoung square-wave voltammetry, square-wave step heights of 1–5 mV, a square amplitude of 15–25 mV with a frequency of 30–240 Hz. All potentials are referenced to decamethylferrocene;  $E_{1/2}$  for sublimed ferrocene was 0.55 V. Infrared and UV/VIS OTTLE data were obtained from standard cells with platinum grid electrodes.

## Preparation of 3–5 via the Sonogashira method

(Trimethylsilyl)acetylene (0.155 ml, 1.1 mmol) was stirred for 24 h at room temperature with **1a** (0.55 g, 1 mmol) and CuI (19 mg, 0.1 mmol) in 20 ml degassed piperidine. The solvent was removed *in vacuo* and the residue separated using column chromatography (alumina/ $\text{CH}_2\text{Cl}_2$ ). The first band eluted was **4**, 53 mg (8%). (Found: C, 41.11; H, 5.11; N, 2.09.  $\text{C}_{22}\text{H}_{31}\text{FeNOPtSSi}$  requires: C, 41.51; H, 4.91; N, 2.20%). Electrospray-MS:  $m/z$  637 ( $\text{M}^+$ ).  $\delta_{\text{H}}(\text{CDCl}_3)$ : 0.17 (s, 9H, Si-CH<sub>3</sub>), 2.97, 3.33 {2 × [s, 3H, Pt satellites ( $J = 39$  Hz), N-CH<sub>3</sub>]}, 3.60, 3.65 {2 × [s, 3H, Pt satellites ( $J = 30$  Hz), S-CH<sub>3</sub>]}, 3.44, 3.77 {2 × [d ( $J = 14$  Hz), 1H, -CH<sub>2</sub>-]}, 4.10 (s, 5H,  $\eta^5\text{-C}_5\text{H}_5\text{Fe}$ ), 4.12 (m, 2H,  $\eta^5\text{-C}_5\text{H}_3\text{Fe}$ ), 4.37 (m, 1H,  $\eta^5\text{-C}_5\text{H}_3\text{Fe}$ ).  $\delta_{\text{Pt}}(\text{CDCl}_3)$ : −3725.  $\nu(\text{KBr}, \text{C}\equiv\text{C}, \text{cm}^{-1})$ : 2172, 2126.

The second band eluted was **3**, 410 mg (67%), crystallized as a yellow-orange solid from benzene–hexane. (Found: C, 39.46; H, 5.05; N, 2.29; S, 4.80.  $\text{C}_{20}\text{H}_{31}\text{FeNOPtSSi}$  requires: C, 39.21; H, 5.10; N, 2.29; S, 5.24%).  $\delta_{\text{H}}(\text{CDCl}_3)$ : 0.12 (s, 9H, Si-CH<sub>3</sub>), 2.95, 3.33 {2 × [s, 3H, Pt satellites ( $J = 39$  Hz), N-CH<sub>3</sub>]}, 3.62, 3.67 {2 × [s, 3H, Pt satellites ( $J = 31$  Hz), S-CH<sub>3</sub>]}, 3.42, 3.81 {2 × [d ( $J = 14$  Hz), 1H, -CH<sub>2</sub>-]}, 4.09 (s, 5H,  $\eta^5\text{-C}_5\text{H}_5\text{Fe}$ ), 4.11 (m, 2H,  $\eta^5\text{-C}_5\text{H}_3\text{Fe}$ ), 4.35 (m, 1H,  $\eta^5\text{-C}_5\text{H}_3\text{Fe}$ ).  $\delta_{\text{Pt}}(\text{CDCl}_3)$ : −3700.  $\nu(\text{KBr}, \text{C}\equiv\text{C}, \text{cm}^{-1})$ : 2034.  $\lambda_{\text{max}}(\text{CH}_2\text{Cl}_2, \text{nm})$ : 251, 288, 465.  $E^{+/0}(\text{CH}_2\text{Cl}_2, \text{V})$ : 0.21.

By a similar procedure **1b** reacted with ethynylferrocene over 1 h to give an orange precipitate of **5** (82%). X-Ray quality crystals were obtained from  $\text{CH}_2\text{Cl}_2$  layered with EtOH. (Found: C, 44.90; H, 4.55; N, 1.89; S, 4.18.  $\text{C}_{27}\text{H}_{31}\text{Fe}_2\text{NOPtS}$  requires: C, 44.77; H, 4.31; N, 1.93; S, 4.43%). Electrospray-MS:  $m/z$  724 ( $\text{M}^+$ ).  $\delta_{\text{H}}(\text{CDCl}_3)$ : 3.02, 3.39 {2 × [s, 3H, Pt satellites ( $J = 38$  Hz), N-CH<sub>3</sub>]}, 3.66, 3.70 {2 × [s, 3H, Pt satellites ( $J = 31$  Hz), S-CH<sub>3</sub>]}, 3.45, 3.82 {2 × [d ( $J = 14$  Hz), 1H, -CH<sub>2</sub>-]}, 4.09, 4.31 [2 × (t, 2H,  $\eta^5\text{-C}_5\text{H}_4\text{Fe}'$ )], 4.13 (s, 5H,  $\eta^5\text{-C}_5\text{H}_5\text{Fe}$ ), 4.15 (m, 2H,  $\eta^5\text{-C}_5\text{H}_3\text{Fe}$ ), 4.17 (s, 5H,  $\eta^5\text{-C}_5\text{H}_5\text{Fe}'$ ), 4.39 (m, 1H,  $\eta^5\text{-C}_5\text{H}_3\text{Fe}$ ).  $\delta_{\text{Pt}}(\text{CDCl}_3)$ : −3700.  $\nu(\text{KBr}, \text{C}\equiv\text{C}, \text{cm}^{-1})$ : 2113, 2097.  $\lambda_{\text{max}}(\text{CH}_2\text{Cl}_2, \text{nm})$ : 237, 287, 456.  $E^{+/0}(\text{CH}_2\text{Cl}_2, \text{V})$ : 0.25, 0.53.

A similar procedure can be used to prepare **6** and is described below.

## Preparation of 6 from 1 using LDA

LDA (0.6 mmol) was added to phenylacetylene (0.9 mmol) in 10 ml THF and the solution stirred for 30 min at room temperature. **1a** (0.55 mmol) dissolved in THF (10 ml) was added and

**Table 2** Crystal data and structure refinement for **3** and **5**

	<b>3</b>	<b>5</b>
Chemical formula	C <sub>26</sub> H <sub>37</sub> NOSiSFePt	C <sub>27</sub> H <sub>31</sub> NO <sub>2</sub> SFe <sub>2</sub> Pt
Formula weight	690.66	740.38
Crystal system	Monoclinic	Monoclinic
Space group	C2/c	C2/c
Absorption coefficient/mm <sup>-1</sup>	5.775	6.315
Final <i>R</i> indices [ <i>I</i> > 2σ( <i>I</i> )] <i>R</i> 1	0.0454	0.0335
<i>wR</i> 2	0.1046	0.0848
<i>R</i> indices (all data) <i>R</i> 1	0.0670	0.0433
<i>wR</i> 2	0.1117	0.0927
Goodness-of-fit on <i>F</i> <sup>2</sup>	0.994	1.014
<i>a</i> /Å	31.9871(6)	29.924(10)
<i>b</i> /Å	10.3174(2)	10.132(3)
<i>c</i> /Å	19.3210(3)	19.366(6)
β/°	120.8720(10)	112.810(7)
<i>V</i> /Å <sup>3</sup>	5472.95(17)	5413(3)
<i>Z</i>	8	8
<i>T</i> /K	153(2)	168(2)
Reflections collected	32062	33369
Independent reflections [ <i>R</i> (int)]	7605 [0.0712]	5535 [0.0380]

the mixture stirred for 12 h. The solvent was removed *in vacuo* and the orange solid separated on preparative silica gel plates (3 : 2; ethylacetate–hexane); work-up of the second band gave an orange powder **6** (20%). Found: C, 44.02; H, 4.56; N, 1.95; S, 4.51. C<sub>23</sub>H<sub>27</sub>FeNOPtS requires: C, 44.80; H, 4.41; N, 2.27; S, 5.20%. FABMS: *m/z* 617 (M<sup>+</sup>). δ<sub>H</sub>(CDCl<sub>3</sub>): 3.02, 3.39 {2 × [s, 3H, Pt satellites (*J* = 39 Hz), N-CH<sub>3</sub>]}, 3.67, 3.71 {2 × [s, 3H, Pt satellites (*J* = 30 Hz), S-CH<sub>3</sub>]}, 3.47, 3.85 {2 × [d (*J* = 14 Hz), 1H, -CH<sub>2</sub>-]}, 4.14 (m, 7H, Fc-*H*), 4.41 (m, 1H, η<sup>5</sup>-C<sub>5</sub>H<sub>5</sub>Fe), 7.16–7.36 (m, 5H, phenyl-*H*). δ<sub>Pt</sub> (CDCl<sub>3</sub>): –3720. ν(KBr, C≡C, cm<sup>-1</sup>): 2100. *E*<sup>+/0</sup> (CH<sub>2</sub>Cl<sub>2</sub>, V): 0.22. When the reaction was repeated using **1b** the yield increased to 45%. **3**, but not **5**, could be prepared in low yield by the same route.

#### Preparation of **8** and **9**

A solution containing **10** (0.05 mmol), trimethylsilylacetylene (0.14 mmol), 2 mol% PdCl<sub>2</sub>(Ph<sub>3</sub>P)<sub>2</sub>/CuI in diisopropylamine (1 ml) was stirred for 3 h at room temperature and then at 50 °C for 2 h. The solvent was evaporated, and the crude brown oil separated on a silica gel column (MeOH–hexane, 7 : 1). The third band was separated on preparative silica gel plates with the same eluent; workup of the first band gave **8**, as yellow crystals (13%). (Found: C, 63.97; H, 7.87; N, 4.31. C<sub>18</sub>H<sub>25</sub>FeNSi requires: C, 63.75; H, 7.43; N, 4.13%). Mass spectrum (EI): 339 (M<sup>+</sup>); 266 (M<sup>+</sup> – (TMS)). δ<sub>H</sub>(CDCl<sub>3</sub>): 0.23, 9H, Si(CH<sub>3</sub>)<sub>3</sub>; 2.21 (s, 6H, 2 × N-CH<sub>3</sub>); 3.49 (s, 2H, CH<sub>2</sub>); 4.11(s, 5H, Cp); 4.15 (t, 1H, 1 × Cp<sup>1</sup>-H); 4.30 (m, 1H, 1 × Cp<sup>1</sup>-H); 4.41 (m, 1H, 1 × Cp<sup>1</sup>-H).

Ethynylferrocene (7.6 mmol) and PdCl<sub>2</sub>(PPh<sub>3</sub>)<sub>2</sub>/CuI (2 mol%) in diisopropylamine were added to **10** (3.8 mmol) and the solution heated under reflux for 16 h. The reaction mixture was then extracted into ether, washed with water, and treated with MgSO<sub>4</sub>. Column chromatography with CH<sub>2</sub>Cl<sub>2</sub> eluted unreacted **10**. Elution with MeOH–hexane–ether (1 : 1 : 1) gave a yellow fraction which was separated on preparative silica gel plates with CH<sub>2</sub>Cl<sub>2</sub>–hexane–MeOH (4 : 2 : 1). Workup of the major orange band gave reddish-brown needles of **9** (53%). (Found: C, 66.47; H, 5.87; N, 3.41. C<sub>25</sub>H<sub>25</sub>Fe<sub>2</sub>N requires: C, 66.55; H, 5.59; N, 3.11%). δ<sub>H</sub>(CDCl<sub>3</sub>): 2.28 (s, 6H, 2 × N-CH<sub>3</sub>); 3.56 (s, 2H, CH<sub>2</sub>); 4.15 (s, 5H, Co); 4.1–4.2 (m, 4H, 3 × Cp<sup>1</sup>-H); 4.23 (s, 5H, Cp); 4.32 (m, 1H, 1 × Cp<sup>1</sup>-H); 4.4–4.5 (m, 2H, 2 × Cp<sup>1</sup>-H). The phenyl analogue **7** could be prepared by the same route.

#### Preparation of **7** from **1a**

LDA (4.5 mmol) was added to a solution of phenylacetylene (1.5 mmol) in THF (20 ml) and the mixture stirred for 30 min at

room temperature. **1a** (1.5 mmol) in THF (15 ml) was added slowly to this solution and the mixture stirred for 8 h. The solvent was removed *in vacuo* and the yellow solid dissolved in dichloromethane. Recrystallisation from ethyl acetate–hexane (1 : 1) gave **7** as a yellow solid in variable yields. (Found: C, 73.52; H, 6.19; N, 4.05. C<sub>21</sub>H<sub>21</sub>FeN requires: C, 73.48; H, 6.17; N, 4.08%). FABMS: *m/z* 343 (M<sup>+</sup>). ν(C≡C, CH<sub>2</sub>Cl<sub>2</sub>, cm<sup>-1</sup>): 2117. δ<sub>H</sub>(CDCl<sub>3</sub>): 2.26 (s, 6H, CH<sub>3</sub>N), 3.56 (s, 2H, CH<sub>2</sub>N), 4.17 (s, 5H, η<sup>5</sup>-C<sub>5</sub>H<sub>5</sub>Fe), 4.21–4.49 (m, 3H, η<sup>5</sup>-C<sub>5</sub>H<sub>5</sub>Fe); 7.33–7.49 (m, 5H, C<sub>6</sub>H<sub>5</sub>).

#### Preparation of **11**

PPh<sub>3</sub> (0.03 mmol) was added to **5** (0.03 mmol) dissolved in CHCl<sub>3</sub> (10 ml) and the solution stirred for 4 h. The solvent was stripped and the product **11** recrystallised from CH<sub>2</sub>Cl<sub>2</sub>–MeOH. Electrospray-MS: *m/z* 908 (M<sup>+</sup>). <sup>1</sup>H NMR δ: 3.26, 3.47 [2 × (d, 3H, <sup>4</sup>J<sub>P-H</sub> = 2 Hz, Pt satellites, N-CH<sub>3</sub>], 3.6 (m, 2H, -CH<sub>2</sub>-), 3.8–3.9 (m, 4H, Fc-*H*), 3.82 (s, 5H, η<sup>5</sup>-C<sub>5</sub>H<sub>5</sub>Fe), 3.89 (s, 5H, η<sup>5</sup>-C<sub>5</sub>H<sub>5</sub>Fe'), 3.89 (t, 2H, η<sup>5</sup>-C<sub>5</sub>H<sub>4</sub>Fe'), 4.07 (m, 1H, η<sup>5</sup>-C<sub>5</sub>H<sub>5</sub>Fe), 7.4 (m, 9H, phenyl-*H*), 7.8 (m, 6H, phenyl-*H*). <sup>195</sup>Pt NMR δ: –4210 (d, *J*<sub>Pt-P</sub> = 4090 Hz) <sup>31</sup>P NMR δ: 16 [Pt satellites (*J* = 4090 Hz)]. ν(KBr, C≡C, cm<sup>-1</sup>): 2074. λ<sub>max</sub> (CH<sub>2</sub>Cl<sub>2</sub>, nm): 293, 465. *E*<sup>+/0</sup> (CH<sub>2</sub>Cl<sub>2</sub>, V): 0.20, 0.48.

#### X-Ray data collection, reduction and structure solution for **3** and **5**

Crystal data for **3** and **5** are given in Table 2. Recrystallisation of **3** from benzene/hexane yielded red plates, one of which was used for data collection. **5** was recrystallised from ethanol as orange-red plates. Data were collected at 153(2) K for **3** and 163(2) K for **5** on a Bruker SMART CCD diffractometer, processed using SAINT,<sup>28</sup> with empirical absorption corrections applied using SADABS.<sup>28</sup> Both structures were solved using SHELXS<sup>28</sup> and refined by full-matrix least-squares using SHELXL-97<sup>28</sup> and TITAN2000.<sup>29</sup> Non-hydrogen atoms were assigned anisotropic temperature factors and the H atoms were included in calculated positions. A difference Fourier synthesis, following the location of all of the non-hydrogen atoms for **3**, revealed six substantial high peaks that could be readily assigned to a benzene solvate molecule in the crystal lattice and refined with isotropic H atoms included in calculated positions. At the same stage of the refinement of **4**, two high peaks remained in the Fourier map. These were assigned to O atoms of water molecules, presumably derived from the ethanol solvent. Refinement of the occupancy factors showed approximately 50% occupancy in each case. These were fixed at 0.5 in the final refinement cycles. No attempt was made to locate the

H atoms for these water molecules. For both structures, anisotropic refinement of the solvates led to a significant reduction in R1. In each refinement, the final difference Fourier maps revealed a number of high peaks close to the Pt atoms but no physical significance could be attached to them.

CCDC reference numbers 159105 and 159106.

See <http://www.rsc.org/suppdata/dt/b1/b101776o/> for crystallographic data in CIF or other electronic format.

## Acknowledgements

We thank Prof. W. T. Robinson (University of Canterbury) for the collection of X-ray data, the University of Otago and the Royal Society (NZ) Marsden Fund for financial support, Robinson College, Cambridge, for a Bye Fellowship (B. H. R.), Amar Flood for assistance with the OTTLE work and Amanda Dixon and Noel Duffy for experimental assistance.

## References

- 1 T. Weyland, C. Lapinte, G. Frapper, M. J. Calhorda, J.-F. Halet and L. Toupet, *Organometallics*, 1997, **16**, 2024; *Conjugated Polymer Materials: Opportunities in Electronic, Optoelectronic and Molecular Electronics*, ed. J. L. Bredas and R. R. Chance, NATO ASI Series, Kluwer, Dordrecht, 1990; vol. 182; I. Manners, *Annu. Rep. Prog. Chem., Sect. A*, 1994, **91**, 131; *Organic Materials for Nonlinear Optics III*, ed. G. J. Ashwell and D. Bloor, Royal Society of Chemistry, Cambridge, 1993, p. 219; H. Lang, *Angew. Chem., Int. Ed. Engl.*, 1994, **33**, 547.
- 2 P. Zanello, in *Ferrocenes*, ed. A. Togni and T. Hayashi, VCH, Weinheim, 1995, ch. 7.
- 3 B. H. Robinson and J. Simpson, in *Paramagnetic Organometallic Species in Activation/Selectivity Catalysis*, ed. M. Chanon, Kluwer, Dordrecht, 1989, p. 357.
- 4 C. E. L. Headford, R. Mason, P. R. Ranatunge-Bandarage, B. H. Robinson and J. Simpson, *J. Chem. Soc., Chem. Commun.*, 1990, 601; P. R. R. Ranatunge-Bandarage, B. H. Robinson and J. Simpson, *Organometallics*, 1994, **13**, 500.
- 5 P. R. R. Ranatunge-Bandarage, S. M. Johnston, N. W. Duffy, B. H. Robinson and J. Simpson, *Organometallics*, 1994, **13**, 511.
- 6 N. W. Duffy, C. J. McAdam, B. H. Robinson and J. Simpson, *Inorg. Chem.*, 1994, **33**, 5343.
- 7 N. W. Duffy, PhD Thesis, University of Otago, 1997.
- 8 H. Paulus, K. Schlögl and H. Weissensteiner, *Monatsh. Chem.*, 1983, **114**, 799.
- 9 H. Plenio, J. Hermann and J. Leukel, *Eur. J. Inorg. Chem.*, 1998, 2063.
- 10 M. C. B. Colbert, J. Lewis, N. J. Long, P. R. Raithby, D. A. Bloor and G. H. Cross, *J. Organomet. Chem.*, 1997, **531**, 183.
- 11 N. W. Duffy, J. Harper, P. R. R. Ranatunge-Bandarage, B. H. Robinson and J. Simpson, *J. Organomet. Chem.*, 1998, **564**, 125.
- 12 L. Fabbrizzi, M. Licchelli and P. Pallavicini, *Acc. Chem. Res.*, 1999, **32**, 846.
- 13 K. McGrouther, D. K. Weston, D. Fenby, B. H. Robinson and J. Simpson, *J. Chem. Soc., Dalton Trans.*, 1999, 1957.
- 14 M. Sato, E. Mogi and S. Kumakura, *Organometallics*, 1995, **14**, 3157.
- 15 K. Tatsumi, R. Hoffmann, A. Yamamoto and J. K. Stille, *Bull. Chem. Soc. Jpn.*, 1981, **54**, 1857.
- 16 M. Pfeffer, J. P. Sutter, M. A. Rotteveel, A. De Cian and J. Fischer, *Tetrahedron*, 1992, **48**, 2427; W. Tao, L. J. Silverberg, A. L. Rheingold and R. F. Heck, *Organometallics*, 1989, **8**, 2550.
- 17 M. Pfeffer, J. P. Sutter, A. De Cian and J. Fischer, *Organometallics*, 1993, **12**, 1167.
- 18 J. Manna, K. D. John and H. D. Hopkins, *Adv. Organomet. Chem.*, 1995, **38**, 79.
- 19 K. Osakada, R. Sakata and T. Yamamoto, *Organometallics*, 1997, **16**, 5354.
- 20 B. Wrackmeyer and K. Horschler, *Prog. Nucl. Magn. Reson. Spectrosc.*, 1990, **22**, 209.
- 21 A. Sebal, C. Stader and B. Wrackmeyer, *J. Organomet. Chem.*, 1986, **311**, 233; J. P. Carpenter and C. M. Lukehart, *Inorg. Chim. Acta*, 1991, **190**, 7; F. Diederich, R. Faust, V. Gramlich and P. Seiler, *J. Chem. Soc., Chem. Commun.*, 1994, 2045; A. Harriman, M. Hissler, R. Ziessel, A. De Cian and J. Fisher, *J. Chem. Soc., Dalton Trans.*, 1995, 4067; S. Leininger, P. J. Stang and S. Huang, *Organometallics*, 1998, **17**, 3981; K. Onitsuka, M. Fujimoto, N. Ohshiro and S. Takahashi, *Angew. Chem., Int. Ed.*, 1999, **38**, 689.
- 22 J. R. Berenguer, E. Fornies, F. Lalinde, E. Martinez, A. J. Urriolabeitia and J. Welch, *J. Chem. Soc., Dalton Trans.*, 1994, 1291; M. Sato, E. Mogi and M. Katada, *Organometallics*, 1995, **14**, 4837; K. Osakada, R. Sakata and T. Yamamoto, *Organometallics*, 1997, **16**, 5354; J. Lewis, N. J. Long, P. R. Raithby, G. P. Shields, W.-Y. Wong and M. Younus, *J. Chem. Soc., Dalton Trans.*, 1997, 4283; W.-Y. Wong, W.-K. Wong and P. R. Raithby, *J. Chem. Soc., Dalton Trans.*, 1998, 2761.
- 23 P. Seiler and J. D. Dunitz, *Acta Crystallogr. Sect. B: Struct. Crystallogr. Cryst. Chem.*, 1979, **35**, 1068.
- 24 M. Spescha, N. W. Duffy, B. H. Robinson and J. Simpson, *Organometallics*, 1994, **13**, 4895.
- 25 S. Barlow and S. R. Marder, *Chem. Commun.*, 2000, 1555.
- 26 T. S. Abram and W. E. Watts, *Synth. React. Inorg. Met.-Org. Chem.*, 1976, **6**, 31.
- 27 M. D. Rausch, A. Siegel and L. P. Klemann, *J. Org. Chem.*, 1966, **31**, 2703.
- 28 SMART (Control) and SAINT (Integration) software, Bruker, AXS, Madison WI, 1994; SADABS, Bruker AXS, Madison WI, 1997; G. M. Sheldrick, SHELXS-96, A program for the solution of crystal structures from diffraction data, 1996, University of Göttingen, Germany; G. M. Sheldrick, SHELXL-97, A program for the refinement of crystal structures, 1997, University of Göttingen, Germany.
- 29 K. A. Hunter and J. Simpson, TITAN2000. A molecular graphics program to aid structure solution and refinement with the SHELX suite of programs, University of Otago, New Zealand, 1999.